NUMERICAL SIMULATION OF LOW CYCLE FATIGUE DAMAGE IN MULTIPHASE MATERIALS

T. Magnin*, O. Madelaine-Dupuich*, A. Bataille† and J. Stolarz*

The physical low cycle fatigue damage of smooth 316L stainless steel, ferritic-pearlitic steel and synthetic Al-12%Si specimens is described at a mesoscopic scale. More than 80% of low cycle fatigue lifetime consists in the development of multiple surface short cracks. High densities of surface cracks, the length of which being lower than the average distance between two propagation barriers (grain boundaries or/and interphase boundaries) favour statistical aspects of their mutual interactions and developments. This gives rise to an approach of low cycle fatigue damage based on statistical physics (accumulation of elementary random damage events) through the development of numerical Monte-Carlo type modelling. Principles and results of the modelling are presented.

INTRODUCTION

The modelling of fatigue damage is still not completely solved. In the low cycle fatigue regime, damage can be described in terms of simultaneously multiple crack nucleation and propagation. In this paper an investigation of fatigue damage process at an intermediate scale (a mesoscopic scale corresponding to the distance between two microstructural barriers) is currently addressed. The importance of the latter scale to model low cycle fatigue lifetimes is pointed out through the physical analysis of fatigue damage and fatigue damage accumulation. During low cycle fatigue, the formation of a dense network of surface microcracks is often observed since very early stages of fatigue tests. The fatigue damage can therefore be described in terms of microcrack initiation and kinetics of surface crack growth as a function of the number of cycles (N/Nr). A computer simulation of low cycle fatigue damage taking into account the microstructural features of the 316L stainless steel alloy has been proposed some years ago by Magnin and Bataille (1). Their low cycle fatigue results on a ferritic-pearlitic alloy support the view that such simulation can be extended to multiphase materials. Indeed in the biphase

* Centre SMS, Ecole des Mines de Saint-Etienne.
† Université des Sciences et Technologies de Lille.

steel (0.4%C) with a regular distribution of both phases, the evolution of surface microcracks follows the same pattern like in 316L (2). The purpose of this paper is 1) to improve the numerical modelling and 2) to extend the simulation of fatigue damage to different multiphase material, particularly a synthetic eutectic Al-Si alloy (AS12) under symmetrical traction-compression.

EVOLUTION OF SURFACE DAMAGE IN LOW CYCLE FATIGUE IN SINGLE PHASE MATERIALS - POSSIBILITIES OF SIMULATION

During low cycle fatigue, first microcracks are created at the slip bands emergence with non-linear interactions of dislocations (microscopic scale). Many experimental results on a 316L stainless steel show that such microcrack initiation takes place at 10% of the fatigue life Nr. The evolution of the surface damage during the remaining 90% consists mainly in nucleation of new microcracks and in coalescence and/or growth of already existing ones. It is convenient to classify the surface microcrack according to their surface length l with respect to the microstructure in relation with the mean grain diameter d_m (mesoscopic scale):

Type I	Type II	Type III	Type IV
$l<d_m$	$d_m<l<3\ d_m$	$3\ d_m<l<10\ d_m$	$10\ d_m<l$

It has been shown that Type I crack nucleation can be considered as an elementary damage event. In a single phase material like 316L, a 2D Monte-Carlo computer simulation of the surface damage in low cycle fatigue has been performed by Magnin and Bataille (1) and gives a relevant correlation between experimental evolution of crack density and predictions (Figure 1a and 1b).

According to their observation, the physical basis of the Coffin Manson law (macroscopic scale) relies on the random character of microcrack nucleation over the whole sample surface and the statistical nature of damage accumulation. This illustrates that randomness at the mesoscopic scale is often the cause of order at the macroscopic scale.

EXPERIMENTAL RESULTS OF LOW CYCLE FATIGUE DAMAGE IN A FERRITIC-PEARLITIC STEEL

Similar mechanism of low cycle fatigue damage have been observed in biphase materials like ferritic-pearlitic steel (2) under assumption that considering orientation and distribution of pearlitic clusters is homogeneous. Short cracks initiate in ferrite phase and steady growth until they meet a transversal ferrite/pearlite interface. Many type I short cracks are stopped at the ferrite/perlite interfaces. However some overcome these microstructural barriers. The second short crack type corresponds to cracks having overcome 2 to 3 ferrite/pearlite interfaces owing to the different local arrangements of pearlite lamellaes

orientation. Therefore, their growth undergoes little influence of the microstructure. Type III considers short cracks longer than 150 μm. The monitoring of populations of these three short crack types at different stages in low-cycle fatigue reveals high crack densities at the surface (figure 2). The presence of several metallurgical phases simply changes the nature of the obstacle to the main crack propagation. The crack number results in a statistical aspect of the damage process. Statistics unifies in this way the description of fatigue damage accumulation in low cycle fatigue.

LOW CYCLE FATIGUE OF A SYNTHETIC Al-12%Si ALLOY RESULTS AND SIMULATION

Low cycle fatigue results

A model eutectic Al-Si alloy has been choosen to understand and simulate the behaviour of multiphase heterogenous alloy which contains one phase in form of platelets. In order to have a good reproductibility of the microstructure, the model Al-Si alloy was manufactured at the Ecole des Mines using an original process in two stages (3). Since no modification has been used, the slightly hypoeutectic structure of AS12 (88.5wt%Al, 11.4wt%Si, 0.1wt%Fe) is composed of Al-Si acicular eutectic and of aluminium dendrites (figure 3a).

The results of low cycle fatigue tests, carried out in tension-compression under symmetrical plastic strain control, at a constant strain rate ($d\varepsilon/dt = 10^{-3}\ s^{-1}$) and in ambient 60% humidity air, are summarized in Table 1 (4).

TABLE 1- AS12 number of cycles to failure at various plastic strain amplitudes.

$\Delta\varepsilon_p/2$	5E-4	1E-3	1.5E-3	2E-3	3E-3
AS12	44000	10300	3800	2660	1120

Analysis of surface crack initiation and propagation . Surface crack initiation takes place exclusively inside eutectic microstructure (no microcracks inside Al dendrites), by fracture of eutectic silicon or Al-Si interfaces. The length of the first microcracks which appear between 5 and 20% of fatigue life is in direct relation with the dimensions of eutectic silicon platelets (about 10 μm). Fatigue damage progresses then through 1) initiation of new microcracks on the surface, 2) propagation in eutectic structure by-passing dendrites and 3) coalescence of microcracks present in neighbouring silicon platelets. The microcracks form a regular network (figure 3b) similar to that observed in steels.

Simulation of fatigue damage of AS12

Description of the mesh. A portion of specimen surface approximately

equal to 0.7 mm^2 is represented by a 2D matrix as shown in figure 4a. The dark lines show the position which corresponds to Si_{eut} square, the large white form corresponds to Al dendrites. The positions of Si_{eut} and Al dendrites are choosen randomly. We define short crack types in the following manner: Type I, short cracks created on eutectic Si particles without any propagation in Al eutectic. First microstructural barriers for the growth of such cracks are Al-Si interfaces. Type II and Type III have the same definition as in 316L with d_m corresponding to the average distance between two microstuctural barriers (Al-Si interfaces).

Nucleation. Only uncracked Si_{eut} unit cell is continously sampled for nucleation. This is a binary-type sampling. A random number is generated and compared to a threshold dependent on plastic strain rate. If the random number value is higher than the threshold value, a short crack will cross every unit cell which corresponds to one Si_{eut} particle. According to the low cycle fatigue damage evolution, crack nucleation is forbidden when few type III short cracks form. This argument is justified by low cycle fatigue results on AS13 where the plastic strain is localized on long cracks since the first quarter of cycle(4).

Surface propagation and surface growth barriers. Every unit cell contiguous to a crack tip except Al dendrite ones is sampled for surface propagation. The Monte Carlo propagation treatment takes place after the nucleation treatment. Thus a random number is generated. It is compared to another threshold which varies according to main parameters: the surface length of short crack, the plastic strain range, the presence of Si particles in the sampled unit cell and the presence of Al dendrites in the sample. The surface short crack propagates unit cell per unit cell. Moreover its propagation processing is uneven from sampling to sampling and uneven when comparing each crack tip. This propagation avoids difficulty in fine speculation about the local physical crack. This Monte Carlo type processing simulates very well the non-continuous and random propagation of short cracks.

Direct crack-crack interactions. The coalescence criterion has been taken from Ochi's results (5). According to his observations, two short cracks are bound to coalesce if their facing tips are less distant than 11% of their total surface length. Coalescence has to participate strongly in the formation of the fatal crack. Moreover a short crack can generate Si particle cracking ahead of its tips.

Short crack growth rate. Short crack growth rates are calculated from experimental data on crack densities as a function of cycle number with use of Tomkins or Mc Clintock type equations (type I and II). Type III surface short cracks exhibit rather different growth behaviour. Their growth rate is considered to be dependent on the plastic strain level and on their surface length.

Calculation of equivalent cycle increment and running procedure. Following

completion of total mesh sampling all changes of short crack surface length are compiled. A new distribution of surface short cracks can then be determined. Every crack belonging to the first and third short crack types is now considered. Type II short cracks are not taken into account for this calculation since they are a link between two short crack types with well-defined growth behaviour. From knowledge of each individual length variation, a mean length increase is calculated for the two-mentionned short crack types. Two equivalent numbers of cycles can be determined, without any confusion between two different propagation mechanisms (short crack growth rate equation). The resulting number of cycles corresponds to cycle increment which is added to the current value of the total number of cycles. Once this is done, the sampling process is run over up to the formation of a 600 microns-surface length short crack. It is assumed that this process predicts the number of cycles to form a type IV short crack for final bulk propagation. The first crack nucleation takes up from 5 to 10% of reduced life N/Ni. Consequently the simulation predicts the following 90-95% of Ni. Simulations can be performed at each plastic strain amplitude giving statitical results including a calculation of standard scatter of crack densities and of predicted lifetime.

Discussion on first results of the numerical simulation. The screen display of simulated specimen surface (figure 4b) shows patterns of crack spatial distribution very similar to experimental ones (figure 3b). Moreover short crack densities are higher than 316L as shown experimentally. Further development of the simulation will take into account texture, orientation of eutectic silicon plates, intersilicium space, interdendrites space, Si particles size and Al dendrites size.

REFERENCES

(1) Bataille, A. and Magnin, T., Acta metall. mater., Vol.42, 1994, p.3817-3825.

(2) Bataille, A. and Magnin, T. "Comparaison of the surface cracking process in uniaxial and multiaxial fatigue", Biaxial/Multiaxial Fatigue Fourth International Conference, Paris, France, 1994.

(3) Madelaine-Dupuich, O., Stolarz, J., Triboulet, G. and Kurzydlowski, K.J. "Solidification processing and microstructure analysis of synthetic Al-Si alloys", ICAA- 5, Grenoble, France, 1996.

(4) Madelaine-Dupuich, O. and Stolarz, J. "Fatigue of eutectic Al-Si alloys", ICAA- 5, Grenoble, France, 1996.

(5) Ochi, Y., Ishii, A. and Sasaki, S.K., Fatigue Fract. Engng Mater. Struct., Vol.8, p.327-335, 1985.

(a) Experimental 316L ($\Delta\varepsilon_p$=0.0008).

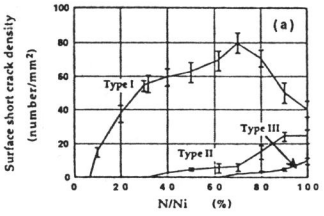

(b)Simulated 316L ($\Delta\varepsilon_p$=0.0008).

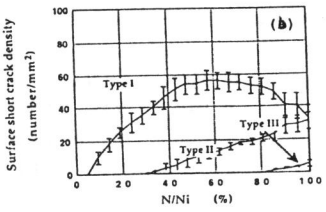

Figure 1 Low-cycle fatigue crack density evolution

(a) a synthetic Al-12%Si.

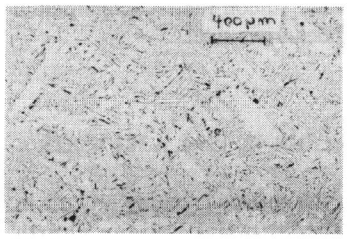

(b) Experimental surface microcracks of AS12 ($\Delta\varepsilon_p$=0.001).

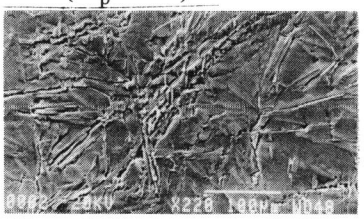

Figure 3 Microstructure of AS12

Ferritic pearlitic steel ($\Delta\sigma$=960MPa).

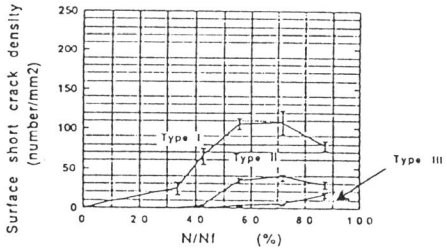

Figure 2 Low-cycle fatigue crack density evolution

(a) initial

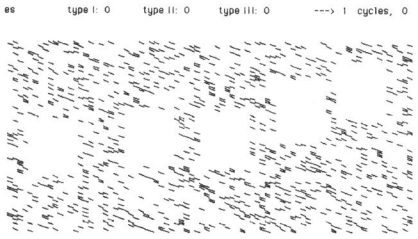

(b) After 11985 simulated cycles.

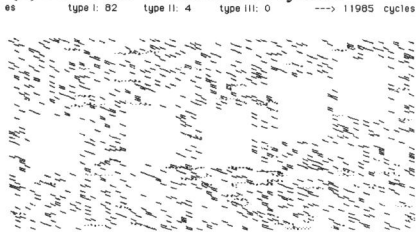

Figure 4 AS12 mesh for simulation ($\Delta\varepsilon_p$=0.0005)